Desalination and Water Treatment
www.deswater.com

doi: 10.5004/dwt.2018.22226

110 (2018) 239–249
April

Large surface area activated carbon from low-rank coal via microwave-assisted KOH activation for methylene blue adsorption

Ali H. Jawad[a,*], Zaman Sahb Mehdi[b], Mohd Azlan Mohd Ishak[c], Khudzir Ismail[a]

[a]*Faculty of Applied Sciences, Universiti Teknologi MARA, 40450 Shah Alam, Selangor, Malaysia, Tel. +60 355211721; Fax: +60355444562; emails: ahjm72@gmail.com, ali288@salam.uitm.edu.my (A.H. Jawad)*
[b]*Chemistry department, College of Science, AL-Muthanna University, Iraq*
[c]*Faculty of Applied Sciences, Universiti Teknologi MARA, 02600 Arau, Perlis, Malaysia*

Received 22 August 2017; Accepted 9 March 2018

ABSTRACT

Merit Kapit (MK) as a low-rank Malaysian coal was utilized as a precursor to develop a large surface area activated carbon (MKAC) via a microwave-induced KOH activation. The characterizations of the raw MK and MKAC were investigated by surface area analysis, scanning electron microscopy, X-ray diffraction, Fourier transform infrared, elemental analysis (CHNS) and point of zero charge (pH_{PZC}) method. The surface area of MKAC was remarkably increased up to 1,100.18 m²/g compared with 332.61 m²/g of MK before activating process. The adsorptive properties of the MKAC with methylene blue (MB) was conducted at different adsorbent dose (0.3–3.6 g/L), solution pH (2–12), initial dye concentrations (25–350 mg/L), contact time (0–240 min) using batch mode operation. The impregnation ratio is 1:2 (MK:KOH), microwave power of 600 W, and radiation time of 15 min resulted in MKAC with a monolayer adsorption capacity of 200 mg/g for MB at 30°C and carbon yield of 63.6%. The kinetic profiles were described by the pseudo-second-order kinetics. Thermodynamic functions indicate a spontaneous and endothermic nature of the adsorption. This study introduces MK as a promising renewable precursor for developing a large surface area activated carbon.

Keywords: Coal; Activated carbon; KOH activation; Microwave irradiation; Adsorption; Methylene blue

1. Introduction

Coal, which results from the physical and chemical alteration of peat (coalification) by processes involving bacterial decay, compaction, heat and time, is an agglomeration of many different complex hydrocarbon compounds [1]. Coal contains a wide variety of organic and mineral phases (mainly hydrogen, sulfur, oxygen, and nitrogen) which varies from one coal deposit to another and from one location to another within the same seam [2]. In Malaysia, coal reserve stands at about 1,712 million tons of various ranks ranging from lignite to anthracite [3]. The total known Malaysia coal area covers about 7,324 km² [4]. Malaysian Merit Kapit coal (MK) is a low-rank coal, mainly located in state Sarawak, East Malaysia. However, the high content of volatile matter, oxygen and moisture in this coal creates difficulties for its wide utilization. The largest coal users in the country are the cement manufacturers and electricity producers. The total consumption of coal at present is about 2.2 million tons per year. The use of coal is relatively new, with some of the cement plants converting from oil to coal in the early 1980's and the commissioning of the only coal fired SSAA power station at Port Kelang in 1989 [5].

Activated carbons (ACs) are materials containing large surface area, well-developed porosity and various functional groups. Therefore, ACs have been widely utilized in versatile applications such as gas separation, solvents recovery, gas storage, super capacitors electrodes, catalyst support, adsorbent for organic and inorganic pollutants from drinking water, and so on [6]. However, a high cost of AC production

* Corresponding author.

limits its application in various technologies. Recognizing this economic obstacle, many investigators have made extensive efforts in low-cost alternatives to activated carbon from a range of carbonaceous precursors, such as lignocellulosic materials [7–10], biopolymer [11], coal [12], char [13], and fruit peels [14]. The textural properties and adsorption capacities of AC mainly depend on the nature of the starting material, activation method, type of activator, and preparation conditions [15,16].

Recently, microwave irradiation has been found to be a rapid and alternative method to prepare, modify, and regenerate AC materials. In this technique, heat is produced within the carbon particle since the energy is directly supplied at the molecular level scale through dipole rotation and ionic conduction [10,16]. By comparing with other conventional activation methods, microwave radiation has rapid temperature rise, uniform temperature distribution, and lower time and energy demands [17]. KOH is widely used in the preparation of AC from many types of carbonaceous precursors due to its many desirable properties such as effectiveness in production of AC with narrow pore size distribution and well-developed porosity, in addition to the eco-friendly property of KOH [18]. Nowadays, interests are growing in the use of other low-cost and locally available coal as raw precursors and steady source for the preparation of large surface area AC.

To the best of our knowledge, development of a large surface area and low-cost activated carbon from low-rank Malaysian coal has not yet been investigated. Therefore, this work aims first to prepare a low-cost activated carbon with a large surface area from locally available Merit Kapit coal (MK) by union of microwave-supported KOH activation, and second, to evaluate the adsorptive properties of received activated carbon (MKAC) for removal of cationic dyes from aqueous solutions. Methylene blue (MB) was chosen as a probe in this study due to its complicated chemical structure and because it is not easy to be removed from wastewater by conventionally used techniques such as biological treatments and chemical precipitation [19,20]. Furthermore, adsorption technique provides high performance and convenience of operation and selectivity as well as exhibits a simple design and flexibility [21,22]. The prepared MKAC was characterized through pore structural analysis (BET), scanning electron microscopy (SEM-EDX), X-ray diffraction (XRD), Fourier transform infrared (FTIR), elemental analysis (CHN), and point of zero charge (pH_{PZC}) method.

2. Experimental section

2.1. Chemicals

MB dye (chemical formula: $C_{16}H_{18}ClN_3S_3H_2O$, molecular weight: 373.9 g/mol, purity 82%, solubility in water: 40 g/L) purchased from R & M Chemicals Company, Malaysia, and used as the adsorbate without any purification. Potassium hydroxide (KOH; HmbG Chemicals, Germany) was used as the chemical reagent for activation. Other chemicals such as hydrochloric acid (HCl) and sodium hydroxide (NaOH) were of analytical grade quality and were purchased from different renowned suppliers.

2.2. Preparation of activated carbon

Merit Kapit low-rank coal (MK) originated from the state Sarawak of East Malaysia was selected as a precursor in this work. The coal samples were ground and sieved to 0.5–0.85 mm. Raw MK was washed and rinsed with hot distilled water to eliminate adherents and until the filtered water was clear. MK was then dried in a vacuum oven for 24 h. The MK coal activated carbon (MKAC) was prepared by mixing KOH with a coal/KOH impregnation ratio of 1:2 (w/w%) with occasional stirring (predetermined as an optimum mixing ratio by taking highest recorded iodine number). The sample was activated by using a quartz glass reactor (7.5 cm diameter and 8.5 cm length) sealed at the bottom and open from the top side to allow the escape of pyrolysis gases. Pyrolysis of sample was carried out in a modified microwave oven (model Panasonic NNJ-993) with a fixed power of 600 W for 20 min in the presence of nitrogen gas (99.995%) at frequency of 2,450 MHz (the irradiation power and time of activation were pre-determined as optimum activation conditions). A schematic illustration of the microwave-assisted pyrolysis system was fully described by our previous published work [23]. The activated products were then cooled down to room temperature and washed with 0.1 M HCl solution and hot distilled water until the filtrate reached a neutral pH value. The produced activated carbon was designated as MKAC, which was then dried in an oven at 100°C for 24 h. The MKAC was stored in tightly closed bottles for further applications. The percent yield of the MKAC was calculated by Eq. (1):

$$\text{Yield (\%)} = \frac{\text{Weight of MKAC}}{\text{Weight of dried MK}} \times 100 \quad (1)$$

2.3. Samples characterization

The iodine number indicates the porosity of the activated carbon and it is defined as the amount of iodine adsorbed by 1 g of carbon at the milligram level, which was determined by standard method [24]. Ultimate analyses of the samples were measured for determining C, H, N, and S content by CHNS-O Analyzer (Flash 2000, Organic Elemental Analyzer, Thermo Scientific, Netherlands). The oxygen contents were calculated by difference. XRD analysis was performed on coal in order to determine the crystallinity or amorphous nature before and after activating process by XRD in reflection mode (Cu K_α radiation) on a PANalytical (UK), X'Pert Pro X-ray diffractometer. Scans were recorded with a scanning rate of 0.59°/s. The diffraction angle (2θ) was varied from 10° to 90°. Textural characterization of the MK and MKAC were carried out by N_2 adsorption using Micromeritics ASAP 2060, USA. FTIR spectral analysis of samples was performed on Spectrum One (PerkinElmer, USA) in the 4,000–500 cm^{-1} wavenumber range. The pellet for infrared studies was prepared by mixing a given sample with KBr crystals and pressed into a pellet. From these FTIR spectra, the presence of surface functional groups before and after activation and adsorption were confirmed. The surface physical morphology was examined by using SEM (JSM-6460LA, JEOL, Japan) technique. The samples were placed on carbon tapes, and then coated with a thin layer of gold–palladium in an argon atmosphere using agar sputter coater. The pH at the point of zero charge (pH_{PZC}) was

estimated using a pH meter (Metrohm, Model 827 pH Lab, Switzerland), as described elsewhere [18].

2.4. Batch adsorption experiments

The batch adsorption experiments of MB onto MKAC were performed in a series of 250 mL Erlenmeyer flasks containing 200 mL of MB solution. The flasks were capped and agitated in an isothermal water bath shaker (waterbath, model WNB7-45, Memmert, Germany) at a fixed shaking speed of 90 strokes/min and 30°C until equilibrium was achieved. Batch adsorption experiments were carried out on common variables of interest such as adsorbent dosage (0.2–3.6 g/L), pH (2–12), initial dye concentration (25–350 mg/L), and contact time (0–240 min) to determine the optimum conditions for dye sorption. The pH of MB solution was adjusted by adding either 0.10 M HCl or NaOH to the desired pH value by monitoring with a pH meter (model 827 pH Lab, Metrohm, Switzerland). After the stirring, the supernatant was collected with a 0.20 μm nylon syringe filter and the concentrations of MB were monitored at a different time interval using a HACH DR 2800 Direct Reading Spectrophotometer at a wavelength of 661 nm. The adsorption capacity at equilibrium, q_e (mg/g) and the percent of color removal, CR (%) of MB were calculated using Eqs. (2) and (3), respectively:

$$q_e = \frac{(C_o - C_e)V}{W} \quad (2)$$

$$\text{CR}\,\% = \frac{(C_o - C_e)}{C_o} \times 100 \quad (3)$$

where C_o is the initial dye concentration (mg/L); C_e is the dye concentration at equilibrium (mg/L); V is the volume of dye solution used (L); and W is the dry mass of the adsorbent used (g). Adsorption experiments were conducted in duplicates and are reported as average values.

3. Results and discussion

3.1. Samples characterization

3.1.1. Surface characteristics

Nitrogen adsorption/desorption curve offers qualitative information on the adsorption mechanism and porous structure of the carbonaceous materials. Fig. 1 shows the N_2 adsorption/desorption isotherm of both MK and MKAC at 77 K with their corresponding pore-size distribution. Based on Fig. 1(a), the initial part of the type IV isotherm is attributed to monolayer–multilayer adsorption. Type IV isotherm is typical for mesoporous materials showing hysteresis loop, which is associated with capillary condensation. The type H3 loop, does not exhibit any limiting adsorption at high P/P_o, is observed with aggregates of plate-like particles giving rise to slit-shaped pores [25]. On the other hand, Fig. 1(c) shows type I isotherm as concave to the P/P_o axis and

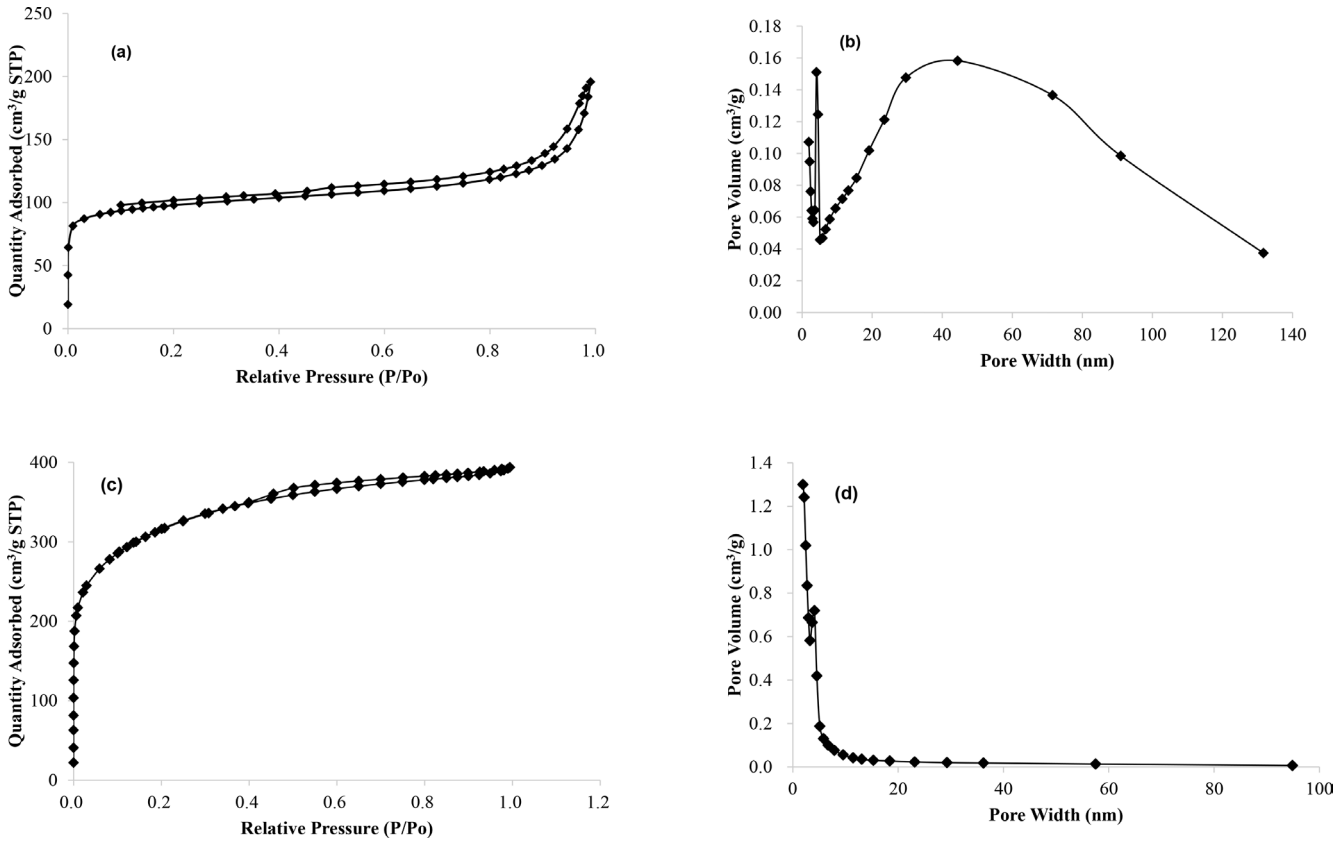

Fig. 1. Isotherms of N_2 adsorption/desorption of MK (a) and MKAC (c), pore-size distribution of MK (b) and MKAC (d).

approaches a limiting value as $P/P_o = 1$. The isotherms display an abrupt increase in adsorbed volume at a low relative pressure (P/P_o). Type I isotherms are given by microporous solids having relatively small external surfaces and the limiting uptake being governed by the accessible micropore volume rather than by the internal surface area. Type I isotherms do not display an apparent desorption hysteresis loop, in accordance with IUPAC classification [25]. Furthermore, the textural parameters of raw MK and MKAC are recorded in Table 1. From Table 1, MKAC can be considered porous material with large BET surface area of 1,100.18 m^2/g compared with less porous raw MK with a relatively low surface area of 332.61 m^2/g. Thus, the KOH activator was responsible for obvious increase in the surface area, which is ~3.3 times greater than raw precursor MK. The development of porosity of activated carbon by KOH activation was associated with gasification according to the following reaction [26]:

$$2KOH \rightarrow K_2O + H_2O$$

$$C + H_2O \rightarrow H_2 + CO$$

$$CO + H_2O \rightarrow H_2 + CO_2$$

$$K_2O + CO_2 \rightarrow K_2CO_3$$

$$K_2O + H_2 \rightarrow 2K + H_2O$$

$$K_2O + C \rightarrow 2K + CO$$

Thus, MKAC with a relatively high yield of 63.6% (Table 1) from MK is obtained from an activation process with KOH. Furthermore, the high iodine number of 1,007 mg/g (Table 1) further confirms that this activated carbon (MKAC) has a large surface area. In fact, a large surface area of MKAC (1,100.18 m^2/g) obtained by this work is higher than other activated carbons obtained by KOH activation from other lignocellulosic materials such as pine apple peel (1,006 m^2/g) [27], palm shell (895 m^2/g) [28], oil palm empty fruit bunch (807.54 m^2/g) [29], rice husk (752 m^2/g) [30], and cotton stalk (729 m^2/g) [31], oil palm fibers (707.79 m^2/g) [32], and pistachio nut shells [33]. Therefore, MK is a promising precursor for the production of high surface area activated carbon.

Table 1
Physicochemical characteristics of the MK and MKAC

Typical properties	Sample	
	MK	MKAC
Single point surface area (m^2/g) at $P/P_o = 0.300$	307.17	1,012.57
BET surface area (m^2/g)	332.61	1,100.18
Langmuir surface area (m^2/g)	442.33	1,486.86
Iodine number (mg/g)	322	998.76
Fixed carbon (yield %)		63.6
Ultimate analysis (wt%)		
C (%)	60.13	71.52
H (%)	1.85	1.14
N (%)	28.39	4.45
S (%)	ND	ND
O[a] (%)	9.63	22.89
C/H	32.50	62.74
C/N	2.12	16.07

ND, Not detected.
[a]By difference.

3.1.2. Elemental analysis

The elemental compositions (CHN) of the raw MK and MKAC were taken and the results are listed in Table 1. It was obvious from the table that KOH used as an activator has significant influence to produce activated carbon (MKAC) with high ratios of C/H and C/N. In the simultaneous microwave pyrolysis and activation processes, the MK decomposes. As a result of decomposition, volatile matters are released from the carbonaceous product. Therefore, the ratio of C/H (62.74) of MKAC becomes approximately twice as high as (32.50) of MK as shown in Table 1. In fact, KOH plays a decisive role for the coal matrix modification. Under the microwave irradiation, metallic potassium is produced and they are intercalated to the carbon matrix, which are responsible for further carbon gasification and release of gaseous products such as CO_2, CO, and H_2 [34].

3.1.3. X-ray diffraction analysis

X-ray computed tomography has applicability over a wide range of applications related to coal structure, behavior, and use. Thus, the XRD pattern of the raw MK and MKAC are shown in Figs. 2(a) and (b), respectively. XRD pattern of MK shows broad peak at 25°, which is an indicative of amorphous nature of the sample. Sharp diffraction peaks from (002), (101), (004), and (103) planes of the crystalline carbon phase are indexed based on the reference pattern. The XRD pattern of the MKAC was quite similar to that of the raw MK. They both had approximately similar number of peaks, except the diffraction pattern of MKAC which showed sharper and intense peaks. From this observation,

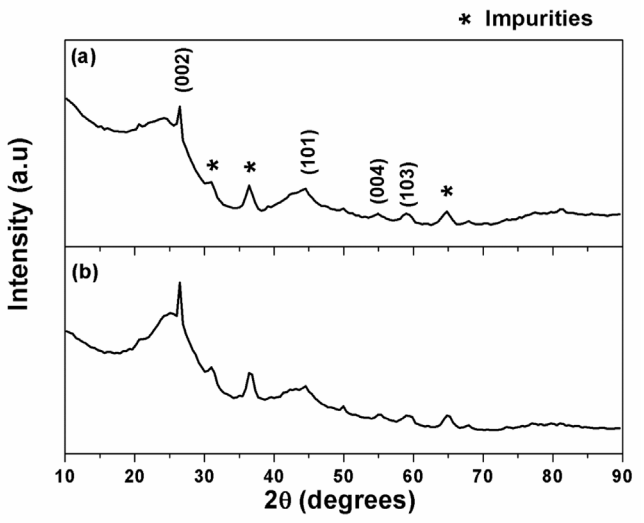

Fig. 2. XRD patterns for MK (a) and MKAC (b).

it can be concluded that the crystal structure of the MKAC was the same as that of the raw MK. This further confirms that the activation process with KOH did not damage the fundamental structure of the raw MK. Similar observation was reported by preparing activated carbon nanotubes by using KOH activation [35].

3.1.4. Surface morphology analysis

SEM analyses of raw MK, MKAC, and MKAC-MB after adsorption of MB are shown in Figs. 3(a)–(c), respectively. As can be seen in Fig. 3(a), the raw MK surface is heterogeneous, irregular, with few visible cavities on it. After chemical activation with KOH (Fig. 3(b)), the MKAC surface appears to be highly porous and heterogeneous. Pores with different size and shape are also clearly visible. The pores are generated due to KOH activator, which was responsible for the porosity development of the raw precursor by creating new pores. Therefore, the resulting pore structure is suitable for the adsorption of MB within the pore structure of MKAC. This assumption is supported by Fig. 3(c), where the MKAC surface is altered after MB adsorption as evidenced by more dense and less open pores seen on the surface of MKAC.

3.1.5. FTIR spectral analysis

Fig. 4 shows the FTIR spectra of (a) MK, (b) MKAC, and (c) MKAC after MB adsorption. As can be seen from Fig. 4(a), the broad bands at 3,500 cm^{-1} is ascribed to the stretching

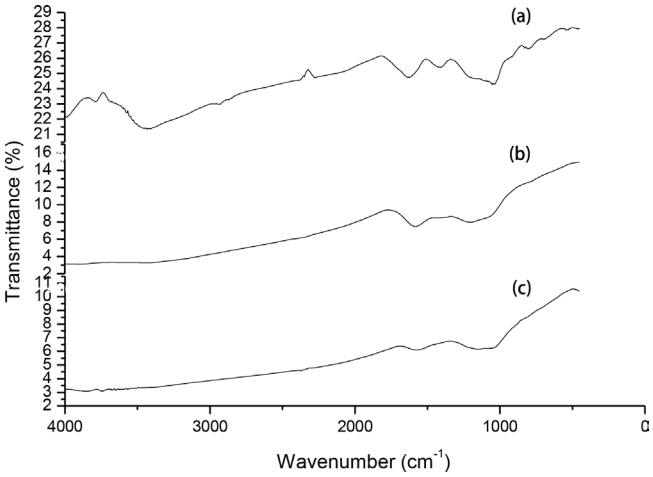

Fig. 4. FTIR spectra for MK (a), MKAC (b), and MKAC after MB adsorption (c).

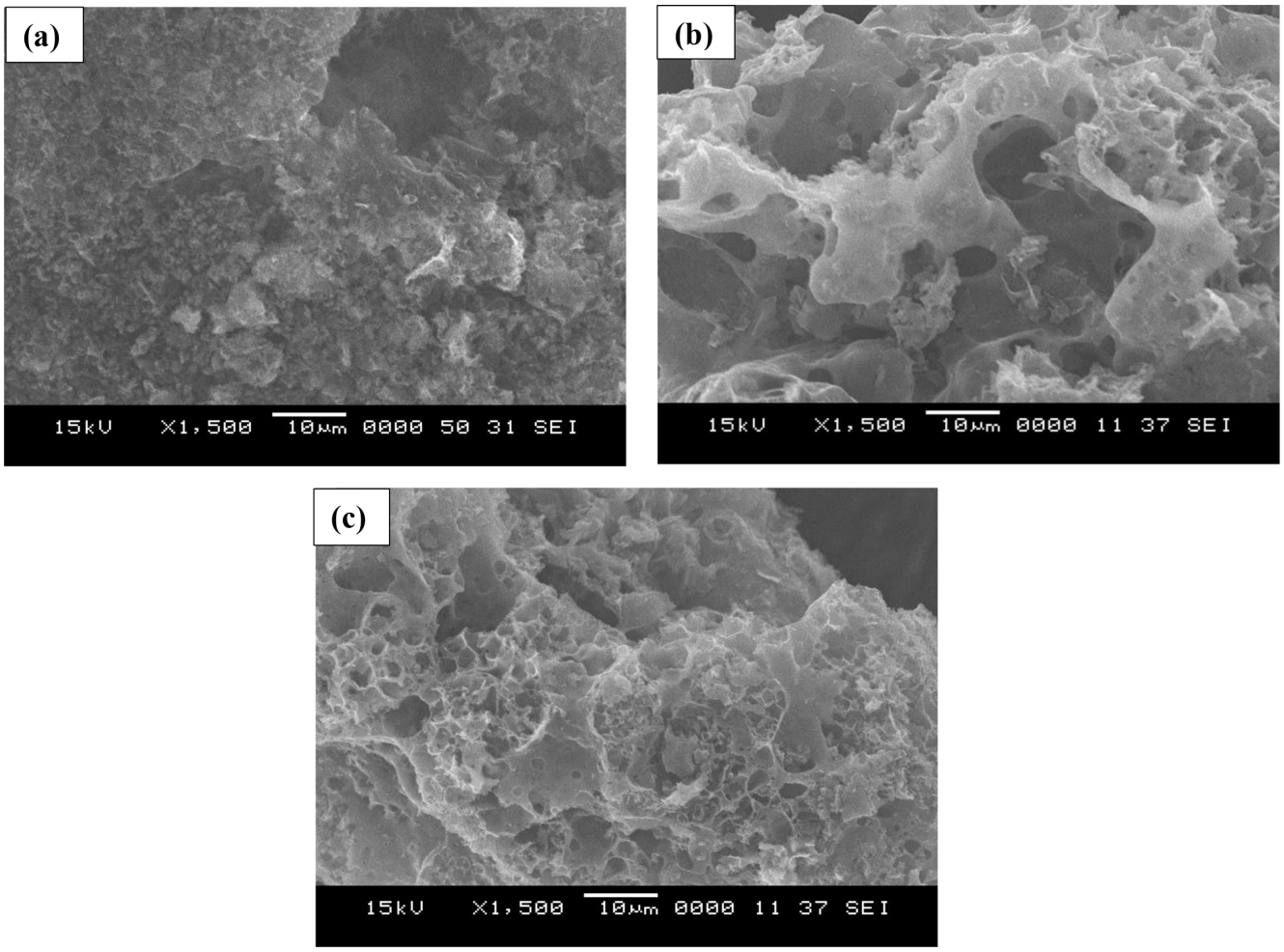

Fig. 3. SEM-EDX profiles for MK (a), MKAC (b), and MKAC after MB adsorption at magnification power of 1,500 K (c).

vibration of hydrogen-bonded hydroxyl (–OH) groups, which indicate the presence of carboxyl, phenol or alcohol groups on the surface of MK [36]. The band at ~1,650 cm^{-1} is ascribed to the stretching vibration of C=O in amide group, amide I [37]. The band at ~1,350–1,300 cm^{-1} is ascribed to methyne C–H bending [38]. The band at 1,000–1,300 cm^{-1} is usually assigned to C–O stretching in acids, alcohols, phenols, ethers, and/or esters groups [39]. The bands at 750–600 cm^{-1} are assigned to alcohol, OH out-of-plane bend [38]. The evidence obtained from Fig. 4(b) indicates that there is an obvious change in the band intensity of (–OH) and slight change in band intensity of (C=O) which are ascribed to the catalytic breaking of these bonds (oxygen–hydrogen–carbon bonds) via activation process with KOH. After MB adsorption (Fig. 4(c)), not much difference can be observed compared with sample before adsorption (Fig. 4(b)), except slight reduction in the band intensities and also little shifting in some bands frequency which might be attributed to interactions with MB cations are the O–H and –COOH Lewis base functional groups.

3.2. Batch adsorption studies

3.2.1. Effect of adsorbent dosage

The effect of MKAC dosage on the amount of MB adsorbed was determined by incubating 100 mL of MB solution with an initial dye concentration of 100 mg/L with the adsorbent, for a contact time of 60 min at 30°C, 110 strokes/min, and an unadjusted pH of 5.60 for the initial MB solution. Variable dosage amounts of MKAC (0.03–0.36 g) were added to the MB solution. Fig. 5 shows the percentage of MB removal increased from 48.6% to 99.6% by increasing the MKAC dosage from 0.03 to 0.12 g. The increase in the percentage of dye removal with adsorbent dosage may relate to an increase in the adsorbent surface area, augmenting the number of adsorption sites available [40]. Therefore, 0.12 g/100 mL was selected as an optimum MKAC dosage for the present study.

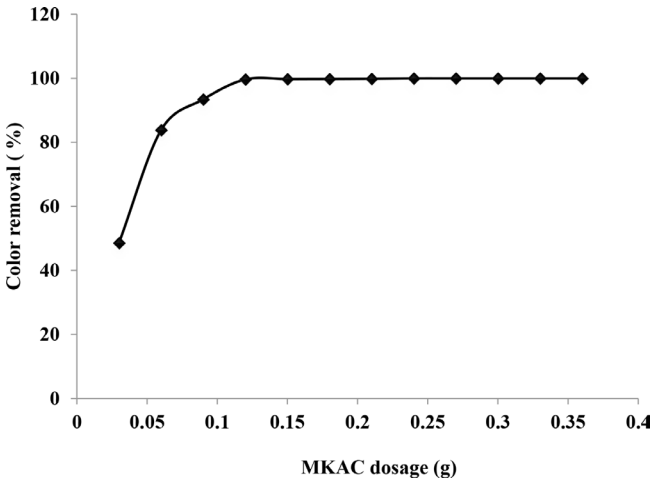

Fig. 5. Effect of MKAC dose on color removal of MB ($[MB]_o$ = 100 mg/L, V = 100 mL, pH = 5.6, shaking speed = 110 strokes/min, temperature = 30°C, and contact time = 60 min).

3.2.2. Effect of pH

The pH_{PZC} is the pH where the adsorbent net surface charge corresponds to zero, and it offers the possible mechanism about the electrostatic interaction between adsorbent and adsorbate [41]. The pH_{PZC} value of 4.3 was obtained for MKAC as shown in Fig. 6(a), while Fig. 6(b) shows the effect of pH, which ranged from 2 to 12, on MB removal by MKAC at an initial MB concentration of 100 mg/L. The surface of MKAC is negatively charged at the pH 4.3 and above. When the pH is increased (5–12), the surface of MKAC may adopt negative surface charge which enhances adsorption of positively charged MB cations through attractive electrostatic attractions, contributing to an increase in the rate of adsorption [41]. The optimum pH for the removal of MB by MKAC is at pH 5.0–6.0. In this respect, it was found that the pH value of the original MB solution is 5.6 and lies within the optimal pH range. Therefore, the pH value of unadjusted MB solution (pH 5.6) was used for this study.

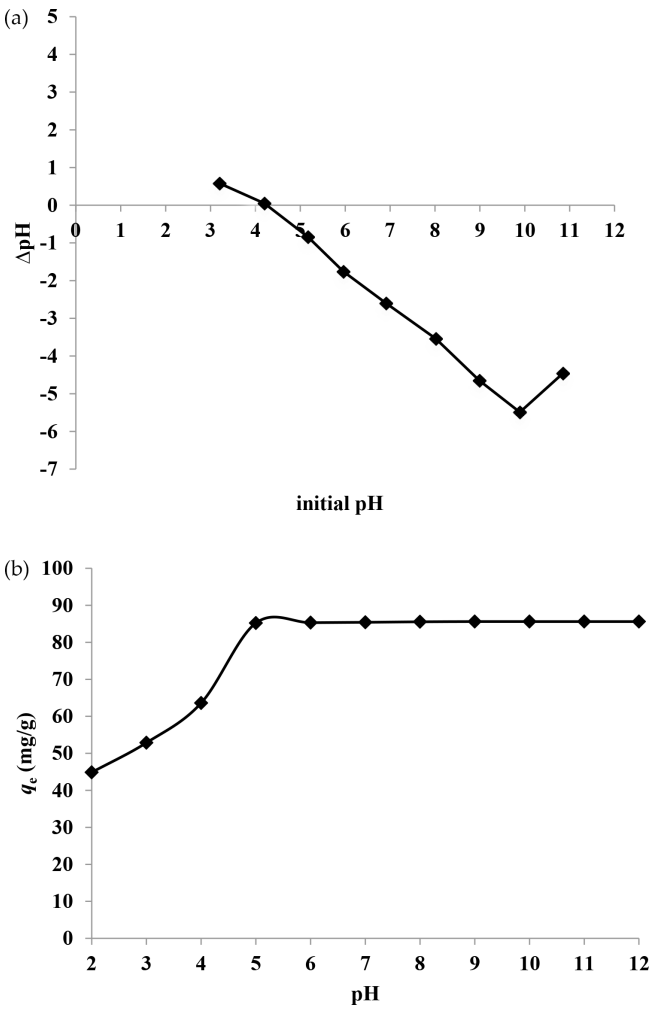

Fig. 6. (a) pH_{PZC} for MKAC suspensions, and (b) effect of pH on MB uptake (mg/g) (MKAC dose = 0.1 g, $[MB]_o$ = 100 mg/L, V = 100 mL, temperature = 30°C, shaking speed = 110 rpm, and contact time = 60 min).

3.2.3. Effect of initial dye concentration and contact time

The effect of adsorption capacity with contact time was investigated with the initial MB concentration that ranged from 50 to 350 mg/L, as shown in Fig. 7. The amount of MB adsorbed by MKAC at equilibrium increased rapidly from 40.8 to 177.3 mg/g with an increase of initial MB concentration from 50 to 350 mg/L. This was attributed to an increase of the collision rate between MB cations and MKAC surface at a higher initial dye concentration. Hence, more MB cations were transferred to the MKAC surface. More time was required to reach equilibrium at higher levels of dye since there was a tendency for MB to penetrate deeper within the interior surface of the MKAC to occupy more active adsorption sites.

3.3. Adsorption isotherm

The adsorption isotherm results for MKAC were fitted using three types of isotherm models, which is Langmuir, Freundlich, and Temkin to evaluate the suitable model for describing the adsorption process. Adsorption isotherm reveals the relationship between the mass of adsorbate adsorbed per unit weight of adsorbent at equilibrium and liquid phase equilibrium concentration of the adsorbate [42,43]. The Langmuir model assumes that the adsorptions occur at specific homogeneous sites on the adsorbent. As well, monolayer adsorption occurs onto a surface containing a finite number of adsorption sites with uniform adsorption and no transmigration of adsorbate on an idealized planar surface. The data of the equilibrium studies for the adsorption of MB dye onto MKAC may follow the Langmuir model [44] as in Eq. (4):

$$\frac{C_e}{q_e} = \frac{1}{q_{\max} k_L} + \frac{1}{q_{\max}} C_e \tag{4}$$

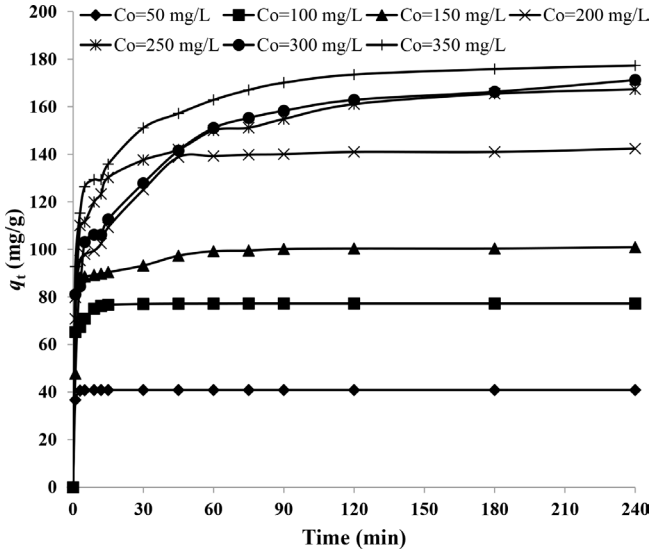

Fig. 7. Effect of initial dye concentration and contact time on the adsorption capacity of MB by MKAC (V = 100 mL, MKAC dose = 0.12 g, pH 5.6, shaking speed = 110 strokes/min, and temperature = 30°C).

where C_e is the equilibrium concentration (mg/L) and q_e is the amount of adsorbed species per specified amount of adsorbent (mg/g), k_L is the Langmuir equilibrium constant, and $q_{\max}$ is the amount of adsorbate required to form an adsorbed monolayer. Hence, a plot of C_e/q_e vs. C_e should be a straight line with a slope ($1/q_{\max}$) and an intercept ($1/q_{\max}.k_L$) as shown in Fig. 8(a). By contrast, the Freundlich model [45] assumes heterogeneous surface energies, as described by a form of the Langmuir equation that varies as a function of the surface coverage. This model is presented as Eq. (5):

$$\ln q_e = \ln k_F + \frac{1}{n} \ln C_e \tag{5}$$

where C_e is the equilibrium concentration of the adsorbate (mg/L), q_e is the amount of adsorbate adsorbed per unit mass of adsorbent (mg/g). The affinity constant k_F ((mg/g)(1/mg)$^{1/n}$), relates to the adsorption capacity of the adsorbent and n is the constant which indicates the relative favorability of the adsorption process. Thus, a plot of ln q_e vs. ln C_e should be a straight line with a slope $1/n$ and an intercept of ln k_F (Fig. 8(b)). Temkin model [46] considered the effects of indirect adsorbate/adsorbate interactions on adsorption isotherms. The Temkin isotherm can be expressed in its linear form as Eq. (6):

$$q_e = B \ln k_T + B \ln C_e \tag{6}$$

where $B = (RT/b)$, a plot of q_e vs. ln C_e yielded a linear line, enables to determine the isotherm constants k_T and B (Fig. 8(c)). k_T is the Temkin equilibrium binding constant (L/mg) that corresponds to the maximum binding energy, and constant B is related to adsorption heat. The adsorption heat of all the molecules in the layer is expected to decrease linearly with coverage because of adsorbate/adsorbate interactions. The related parameters were calculated, and the results are shown in Table 2. Based on calculated data, Langmuir model fits the data better than the Freundlich and Temkin models. This result is confirmed by the high R^2 value for the Langmuir model (0.998) compared with the Freundlich (0.960) and Temkin (0.620) models. Langmuir isotherm indicates the surface homogeneity of the adsorbent. The adsorbent surface is made up of small adsorption patches, which are energetically equivalent to each other in terms of adsorption phenomenon. The monolayer adsorption capacity ($q_{\max}$) for MKAC with MB was 200 mg/g. This result indicates that MK is a promising renewable precursor that can be utilized to develop an efficient porous activated carbon with potential application for uptaking cationic dyes such as MB.

3.4. Kinetic studies

The pseudo-first-order model (PFO) and pseudo-second-order model (PSO) were used to investigate the adsorption kinetics of MB dye on MKAC. The PFO was originally proposed by Lagergren [47] and its linearized form is given by Eq. (7):

$$\ln(q_e - q_t) = \ln q_e - k_1 t \tag{7}$$

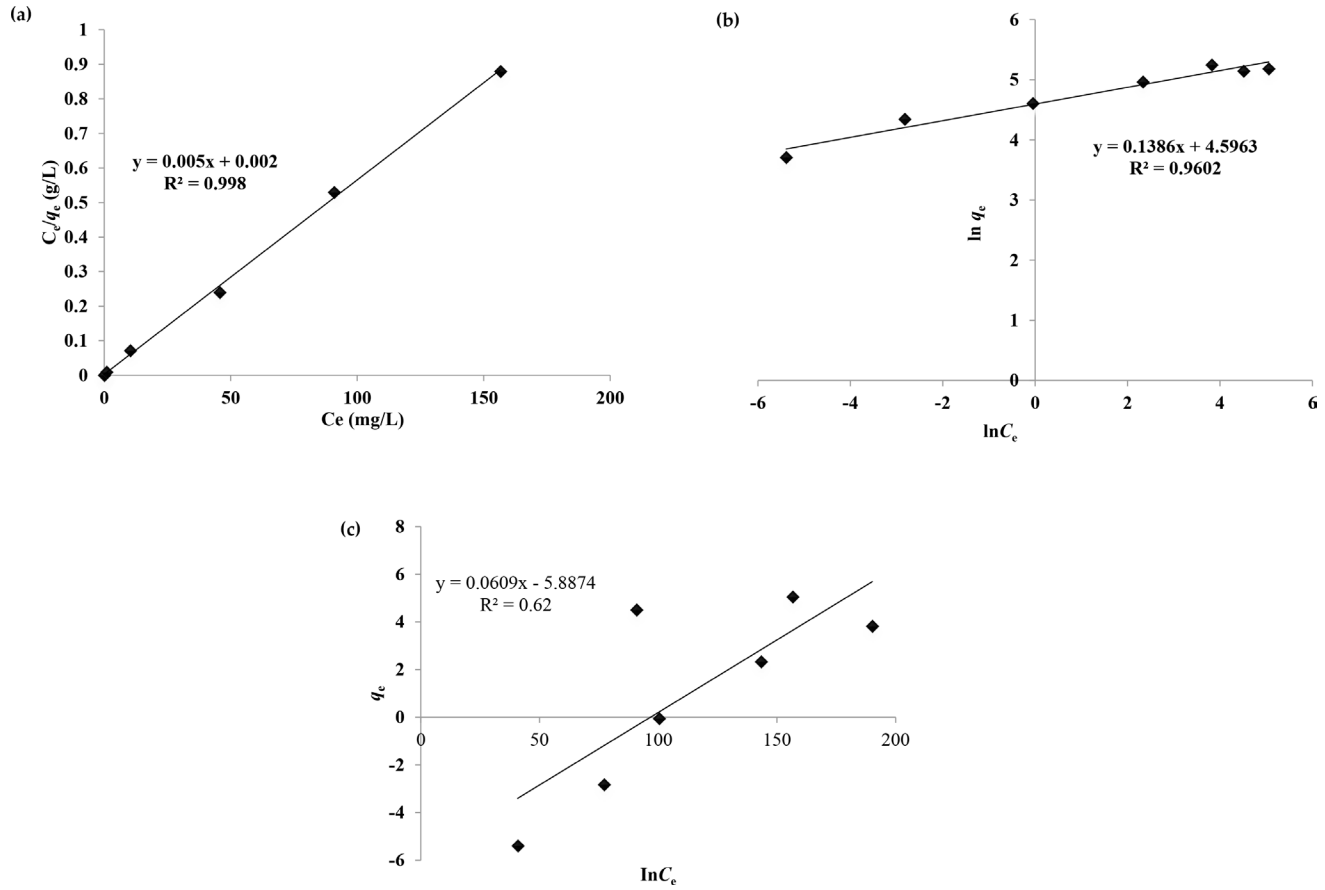

Fig. 8. Adsorption isotherm plots of the Langmuir (a), Freundlich (b), and Temkin (c) models for MB adsorption onto MKAC at 30°C.

Table 2
Parameters of the Langmuir, Freundlich, and Temkin isotherm models for MB adsorption onto MKAC surface at 30°C

Isotherm	Parameter	Value
Langmuir	q_m (mg/g)	200
	K_L (L/mg)	2.5
	R^2	0.998
Freundlich	k_F ((mg/g)(L/mg)$^{1/n}$)	99.09
	N	0.138
	R^2	0.960
Temkin	K_T (L/mg)	4.47
	B	0.061
	R^2	0.620

where q_e is the amount of solute adsorbed at equilibrium per unit weight of adsorbent (mg/g), q_t is the amount of solute adsorbed at any time (mg/g), and k_1 is the adsorption constant. This expression is the most popular form of PFO. k_1 values at different initial MB concentrations were calculated from the plots of ln ($q_e - q_t$) vs. t (Fig. 9(a)) and the values are given in Table 3. The linear form of the PSO is given by Eq. (8) [48]:

$$\frac{t}{q_t} = \frac{1}{k_2 q_e^2} + \frac{t}{q_e} \tag{8}$$

where the PSO is the rate constant (k_2, g/mg min) and $q_{e,\mathrm{cal}}$ were calculated from the intercept and slope of t/q_t vs. t, shown in Fig. 9(b). In Table 3, the observed R^2 values are nearly unity ($R^2 \geq 0.99$) for the PSO, where the values of $q_{e,\mathrm{cal}}$ are in good agreement with $q_{e,\mathrm{exp}}$.

3.5. Adsorption thermodynamics

The thermodynamic adsorption parameters of MB onto MKAC were computed from the experimental data obtained at 313, 323, and 333 K. Gibb's free energy ($\Delta G°$), enthalpy ($\Delta H°$) and entropy ($\Delta S°$) were calculated using the following Eqs. (9)–(11) [49]:

$$k_d = \frac{q_e}{C_e} \tag{9}$$

$$\Delta G° = \Delta H° - T\Delta S° \tag{10}$$

$$\ln k_d = \frac{\Delta S°}{R} - \frac{\Delta H°}{RT} \tag{11}$$

where k_d is the distribution coefficient, q_e is the concentration of MB adsorbed onto MKAC at equilibrium (mg/L), C_e is the equilibrium concentration of MB in the liquid phase (mg/L), R is the universal gas constant (8.314 J/mol K), and T is the

absolute temperature (K). The values of $\Delta H°$ and $\Delta S°$ were calculated from the slope and intercept of van't Hoff plots of ln k_d vs. 1/T, respectively (Fig. 10). The thermodynamic parameters are listed in Table 4. In general, the value for $\Delta G°$, energy for physisorption ranges from –20 to 0 kJ/mol, the physisorption together with chemisorption falls at the range of –20 to –80 kJ/mol and chemisorption is more negative in magnitude with a range of –80 to –400 kJ/mol [50]. The negative values of $\Delta G°$ indicate spontaneous and favorable MB adsorption onto the surface of MKAC [18]. The enthalpy for physisorption is generally below 0 kJ/mol, while for the chemisorption is a more negative range (80–420 kJ/mol) of values [51]. The positive value of the enthalpy change ($\Delta H°$ = 113.34 kJ/mol) indicates that the adsorption process is endothermic and this value also shows that the adsorption follows a chemisorption mechanism in nature involving strong forces of attractions [52]. The positive entropy change ($\Delta S°$) value of 391.80 J/mol K confirms a high preference of MB molecules for the carbon surface of MKAC and also suggests

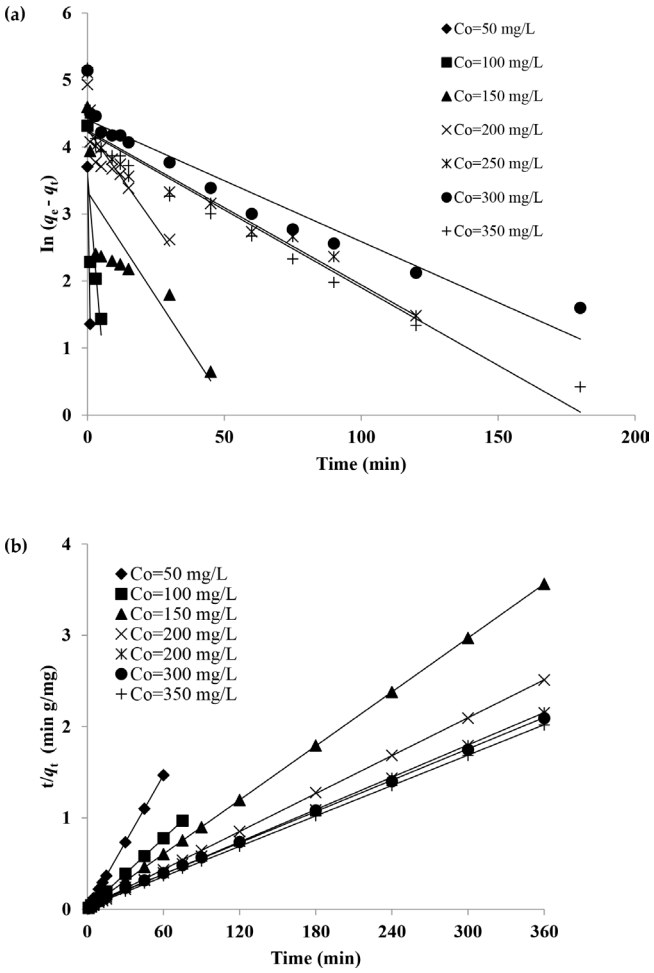

Fig. 9. Kinetic profiles for the adsorption of MB onto MKAC at 30°C: (a) PFO and (b) PSO.

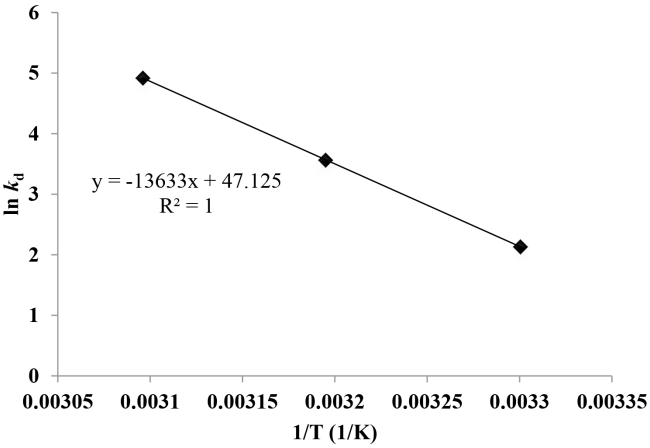

Fig. 10. Plot of ln k_d vs. 1/T for calculation of thermodynamic parameters for the adsorption of MB onto MKAC.

Table 4
Thermodynamic parameter values for the adsorption of MB onto MKAC

Temperature (K)	Thermodynamics			
	k_d	$\Delta G°$ (kJ/mol)	$\Delta H°$ (kJ/mol)	$\Delta S°$ (J/mol K)
313	8.45	–232.12	113.34	391.80
323	35.33	–236.04		
333	137.07	–239.96		

Table 3
Parameters of the PFO and PSO for MB adsorption onto MKAC at different initial MB concentrations at 30°C

Parameters							
C_o (mg/L)	50	100	150	200	250	300	350
$q_{e,exp}$ (mg/g)	41.6	83.3	111.1	166.7	174.6	184.8	204.6
PFO							
$q_{e,meas}$ (mg/g)	40.6	59.5	92.5	123.4	159.2	171.3	189.6
k_1 (min^{-1})	2.35	0.481	0.062	0.058	0.023	0.018	0.016
R^2	0.999	0.727	0.668	0.779	0.880	0.920	0.937
PSO							
$q_{e,meas}$ (mg/g)	40.9	79.8	110.4	162.6	171.7	181.2	201.7
$k_2 \times 10^{-3}$ (g/mg min)	576	48.0	6.23	1.71	0.83	0.61	0.19
R^2	1	1	0.999	0.999	0.998	0.999	0.999

the possibility of some structural changes or readjustments in the dye–carbon adsorption complex. It also corresponds to an increase in the degree of freedom of the adsorbed species due to adsorbate disorder and/or loss of water upon binding of MB onto the MKAC surface.

4. Conclusions

Microwave-assisted KOH activation was used to prepare porous activated carbons. MK low-rank coal was utilized as a low-cost precursor for preparation of a large surface area activated carbon (MKAC). Additionally, the surface area and iodine number of MKAC are 1,100.18 m^2/g and 998.76 mg/g, respectively. The prepared MKAC shows efficient removal for MB from aqueous solution. In this study, equilibrium adsorption data of MB onto MKAC was well represented by Langmuir isotherm model, showing maximum adsorption capacity of 200 mg/g. The adsorption kinetic data were well described by the PSO. Thus, these results indicated that MKAC is a low-cost and an efficient adsorbent for MB adsorption.

Acknowledgments

The authors would like to thank the Faculty of Applied Sciences, Universiti Teknologi MARA for facilitating this work. The authors would also like to thank Dr. Mahesh Kumar Talari for his fruitful discussions on X-ray diffraction analysis.

References

[1] W. Francis, Coal, Its Formation and Composition, 2nd ed., Edward Arnold, London, UK, 1961.
[2] A.S. Azmi, S. Yusup, S. Muhamad, The influence of temperature on adsorption capacity of Malaysian coal, Chem. Eng. Process., 45 (2006) 392–396.
[3] S.S. Idris, N.A. Rahman, K. Ismail, A.B. Alias, Z.A. Rashid, J.A.M.J. Mohd, Investigation on thermochemical behaviour of low rank Malaysian coal, oil palm biomass and their blends during pyrolysis via thermogravimetric analysis (TGA), Bioresour. Technol., 101 (2010) 4584–4592.
[4] A.U. Ambun, Malaysia's Coal Resource: Opportunities and Challenges, Department of Mineral and Geosciences Malaysia, Sarawak, 2003. Available at: http://www.p.sabah.gov.my/galian/N SeminarP123.html (Accessed 8 December 2003).
[5] C.B. Lim, Environmental Protection in Coal Utilization and Its Problems at Sultan Salahuddin Abdul Aziz Power Station, Kapar, National Energy Corporation, 1991.
[6] J. Xu, L. Chen, H. Qu, Y. Jiao, J. Xie, G. Xing, Preparation and characterization of activated carbon from reedy grass leaves by chemical activation with H_3PO_4, Appl. Surface Sci., 320 (2014) 674–680.
[7] A.H. Jawad, R.A. Rashid, K. Ismail, S. Sabar, High surface area mesoporous activated carbon developed from coconut leaf by chemical activation with H_3PO_4 for adsorption of methylene blue, Desal. Wat. Treat., 74 (2017) 326–335.
[8] A.H. Jawad, S. Sabar, M.A.M. Ishak, L.D. Wilson, S.S.A. Norrahma, M.K. Talari, A.M. Farhan, Microwave-assisted preparation of mesoporous activated carbon from coconut (*Cocos nucifera*) leaf by H_3PO_4-activation for methylene blue adsorption, Chem. Eng. Commun., 204 (2017) 1143–1156.
[9] A.H. Jawad, R.A. Rashid, M.A.M. Ishak, L.D. Wilson, Adsorption of methylene blue onto activated carbon developed from biomass waste by H_2SO_4 activation: kinetic, equilibrium and thermodynamic studies, Desal. Wat. Treat., 57 (2016) 25194–25206.
[10] A.H. Jawad, M.A.M. Ishak, A.M. Farhan, K. Ismail, Response surface methodology approach for optimization of color removal and COD reduction of methylene blue using microwave-induced NaOH activated carbon from biomass waste, Desal. Wat. Treat., 62 (2017) 208–220.
[11] F. Marrakchi, M.J. Ahmed, W.A. Khanday, M. Asif, B.H. Hameed, Mesoporous-activated carbon prepared from chitosan flakes via single-step sodium hydroxide activation for the adsorption of methylene blue, Int. J. Biol. Macromol., 98 (2017) 233–239.
[12] L. Gao, F. Dong, Q. Dai, G. Zhong, U. Halik, D. Lee, Coal tar residues based activated carbon: preparation and characterization, J. Taiwan Inst. Chem. Eng., 63 (2016) 166–169.
[13] R. Acosta, V. Fierro, A.M. Yuso, D. Nabarlatz, A. Celzard, Tetracycline adsorption onto activated carbons produced by KOH activation of tyre pyrolysis char, Chemosphere, 149 (2016) 168–176.
[14] A.H. Jawad, N.F.H. Mamat, M.F. Abdullah, K. Ismail, Adsorption of methylene blue onto acid-treated mango peels: kinetic, equilibrium and thermodynamic, Desal. Wat. Treat., 59 (2017) 210–219.
[15] E. Yagmur, M. Ozmak, Z. Aktas, A novel method for production of activated carbon from waste tea by chemical activation with microwave energy, Fuel, 87 (2008) 3278–3285.
[16] Q.S. Liu, T. Zheng, N. Li, P. Wang, G. Abulikemu, Modification of bamboo-based activated carbon using microwave radiation and its effects on the adsorption of methylene blue, Appl. Surf. Sci., 256 (2010) 3309–3315.
[17] X. Wang, X. Liang, Y. Wang, X. Wang, M. Liu, D. Yin, Y. Zhang, Adsorption of copper (II) onto activated carbons from sewage sludge by microwave-induced phosphoric acid and zinc chloride activation, Desalination, 278 (2011) 231–237.
[18] R.A. Rashid, A.H. Jawad, M.A.M. Ishak, N.N. Kasim, KOH-activated carbon developed from biomass waste: adsorption equilibrium, kinetic and thermodynamic studies for Methylene blue uptake, Desal. Wat. Treat., 57 (2016) 27226–27236.
[19] F. Aci, M. Nebioglu, M. Arslan, M. Imamoglu, M. Zengin, M. Kuecuekislamoglu, Preparation of activated carbon from sugar beet molasses and adsorption of methylene blue, Fresenius Environ. Bull., 17 (2008) 997–1001.
[20] A.H. Jawad, A.F. Alkarkhi, N.S.A. Mubarak, Photocatalytic decolorization of methylene blue by an immobilized TiO_2 film under visible light irradiation: optimization using response surface methodology (RSM), Desal. Wat. Treat., 56 (2015) 161–172.
[21] A.H. Jawad, M.A. Islam, B.H. Hameed, Cross-linked chitosan thin film coated onto glass plate as an effective adsorbent for adsorption of reactive orange 16, Int. J. Biol. Macromol., 95 (2017) 743–749.
[22] N.S.A. Mubarak, A.H. Jawad, W.I. Nawawi, Equilibrium, kinetic and thermodynamic studies of Reactive Red 120 dye adsorption by chitosan beads from aqueous solution, Energy Ecol. Environ., 2 (2017) 85–93.
[23] M.A. Jamaluddin, K. Ismail, M.A.M. Ishak, Z. Ab Ghani, M.F. Abdullah, M.T.U. Safian, N.I.N. Mohd Hakimi, Microwave-assisted pyrolysis of palm kernel shell: optimization using response surface methodology (RSM), Renew. Energy, 55 (2013) 357–365.
[24] M. Ahmedna, W.E. Marshall, R.M. Rao, S.J. Clarke, Use of filtration and buffers in raw sugar colour measurements, J. Sci. Food Agric., 75 (1997) 109–116.
[25] K.S.W. Sing, D.H. Everett, R.A.W. Haul, L. Moscou, R.A. Pierotti, J. Rouquerol, T. Siemienewska, Reporting physisorption data for gas–solid systems, Pure Appl. Chem., 57 (1985) 603–619.
[26] Y. Guo, K. Yu, Z. Wang, H. Xu, Effects of activation conditions on preparation of porous carbon from rice husk, Carbon, 41 (2000) 1645–1687.
[27] K.Y. Foo, B.H. Hameed, Porous structure and adsorptive properties of pineapple peel based activated carbons prepared via microwave assisted KOH and K_2CO_3 activation, Microporous Mesoporous Mater., 148 (2012) 191–195.
[28] K.Y. Foo, B.H. Hameed, Utilization of oil palm biodiesel solid residue as renewable sources for preparation of granular

activated carbon by microwave induced KOH activation, Bioresour. Technol., 130 (2013) 696–702.
[29] K.Y. Foo, B.H. Hameed, Preparation of oil palm (Elaeis) empty fruit bunch activated carbon by microwave-assisted KOH activation for the adsorption of methylene blue, Desalination, 275 (2011) 302–305.
[30] K.Y. Foo, B.H. Hameed, Utilization of rice husks as a feedstock for preparation of activated carbon by microwave induced KOH and K_2CO_3 activation, Bioresour. Technol., 102 (2011) 9814–9817.
[31] H. Deng, G. Li, H. Yang, J. Tang, J. Tang, Preparation of activated carbons from cotton stalk by microwave assisted KOH and K_2CO_3 activation, Chem. Eng. J., 163 (2010) 373–381.
[32] K.Y. Foo, B.H. Hameed, Microwave-assisted preparation of oil palm fiber activated carbon for methylene blue adsorption, Chem. Eng. J., 166 (2011) 792–795.
[33] K.Y. Foo, B.H. Hameed, Preparation and characterization of activated carbon from pistachio nut shells via microwave-induced chemical activation, Biomass Bioenergy, 35 (2011) 3257–3261.
[34] J. Laine, A. Calafat, Factors affecting the preparation of activated carbons from coconut shell catalized by potassium, Carbon, 29 (1991) 949–953.
[35] Q. Jiang, M.Z. Qu, G.M. Zhou, B.L. Zhang, Z.L. Yu, A study of activated carbon nanotubes as electrochemical super capacitors electrode materials, Mater. Lett., 57 (2002) 988–991.
[36] M.D. Pavlović, A.V. Buntić, K.R. Mihajlovski, S.S. Šiler-Marinković, D.G. Antonović, Ž. Radovanović, S.I. Dimitrijević-Branković, Rapid cationic dye adsorption on polyphenol-extracted coffee grounds—a response surface methodology approach, J. Taiwan Inst. Chem. Eng., 45 (2014) 1691–1699.
[37] A.H. Jawad, M.A. Nawi, Characterizations of the photocatalytically-oxidized cross-linked chitosan-glutaraldehyde and its application as a sub-layer in the TiO_2/CS-GLA bilayer photocatalyst system, J. Polym. Environ., 20 (2012) 817–829.
[38] J. Coates, Interpretation of Infrared Spectra, A Practical Approach, R.A. Meyers, Ed., Encyclopedia of Analytical Chemistry, John Wiley & Sons Ltd., Chichester, 2000, pp. 10815–10837.
[39] M.N. Nawi, A.H. Jawad, S. Sabar, W.S.W. Ngah, Photocatalytic-oxidation of solid state chitosan by immobilized bilayer assembly of TiO_2–chitosan under a compact household fluorescent lamp irradiation, Carbohydr. Polym., 83 (2011) 1146–1152.
[40] B. Hayati, N.M. Mahmoodi, Modification of activated carbon by the alkaline treatment to remove the dyes from wastewater: mechanism, isotherm and kinetic, Desal. Wat. Treat., 47 (2012) 322–333.
[41] M.A. Islam, S. Sabar, A. Benhouri, W.A. Khanday, M. Asif, B.H. Hameed, Nanoporous activated carbon prepared from karanj (*Pongamia pinnata*) fruit hulls for methylene blue adsorption, J. Taiwan Inst. Chem. Eng., 74 (2017) 96–104.
[42] S. Chakraborty, S. Chowdhury, P. Das Saha, Adsorption of Crystal Violet from aqueous solution onto NaOH-modified rice husk, Carbohydr. Polym., 86 (2011) 1533–1541.
[43] M.V. Lopez-Ramon, F. Stoeckli, C. Moreno-Castilla, F. Carrasco-Marin, On the characterization of acidic and basic surface sites on carbons by various techniques, Carbon, 37 (1999) 1215–1221.
[44] I. Langmuir, The adsorption of gases on plane surfaces of glass, mica and platinum, J. Am. Chem. Soc., 40 (1918) 1361–1403.
[45] H. Freundlich, Ueber die adsorption in Loesungen (Adsorption in solution), Z. Phys. Chem., 57 (1906) 385–470.
[46] M.J. Temkin, V. Pyzhev, Recent modifications to Langmuir isotherms, Acta Physiochim. URSS, 12 (1940) 217–222.
[47] S. Lagergren, Zur theorie der sogenannten adsorption geloster stoffe, K. Sven. Vetensk.akad. Handl., 24 (1898) 1–39.
[48] Y.S. Ho, G. McKay, Sorption of dye from aqueous solution by peat, Chem. Eng. J., 70 (1998) 115–124.
[49] G. Karaçetin, S. Sivrikaya, M. Imamoğlu, Adsorption of methylene blue from aqueous solutions by activated carbon prepared from hazelnut husk using zinc chloride, J. Anal. Appl. Pyrolysis, 110 (2014) 270–276.
[50] M.J. Jaycock, G.D. Parfitt, Chemistry of Interfaces, Ellis Horwood Ltd., Onichester, 1981.
[51] K.E. Noll, V. Gounaris, W.S. Hou, Adsorption Technology for Air and Water Pollution Control, Lewis Publishers, Chelsea, MI, 1992, pp. 21–22.
[52] Y. Yu, Y.Y. Zhuang, Z.H. Wang, Adsorption of water-soluble dye onto functionalized resin, J. Colloid Interface Sci., 242 (2001) 288–293.
[53] D.D. Asouhidou, K.S. Triantafyllidis, N.K. Lazaridis, K.A. Matis, S.S. Kim, T.J. Pinnavaia, Sorption of reactive dyes from aqueous solutions by ordered hexagonal and disordered mesoporous carbons, Microporous Mesoporous Mater., 117 (2009) 257–267.